Neodymium fluoride film thickness changes by 7 keV Ar^+ bombardment*

A. Oliver, A. Crespo, J. Miranda and E. Andrade
Instituto de Física
Universidad Nacional Autónoma de México
Apartado postal 20-364, 01000 México, D.F., México

Recibido el 5 de junio de 1992; aceptado el 4 de septiembre de 1992

Abstract. NdF_3 films with thicknesses of 100 $\mu g/cm^2$ and 367 $\mu g/cm^2$ deposited onto carbon substrates were bombarded by a 7 keV Ar^+ beam. Fluences varied from 5×10^{16} ion/cm^2 to 1.9×10^{18} ions/cm^2. The thickness changes produced by the Ar irradiation were measured by Proton Induced X-ray Emission (PIXE) and Resonant Nuclear Reaction Analysis (RNRA). Two sputtering regimes were found for two different film thicknesses.

Resumen. Se bombardearon con un haz de Ar^+ de 7 keV, películas de NdF_3 con espesores de 100 $\mu g/cm^2$ y 367 $\mu g/cm^2$ depositados por evaporación sobre sustratos de carbón. Las afluencias se variaron de 5×10^{16} iones/cm^2 hasta 1.9×10^{18} iones/cm^2. Los cambios en espesor producidos por la irradiación de Ar se midieron por los rayos X inducidos por protones (PIXE) y por reacción nuclear resonante (RNRA). Se encontraron dos razones de erosión iónica para muestras con dos espesores diferentes.

PACS: 82.90.+j; 61.80.Jh

1. Introduction

Metal halides are important technologically because they have a range of useful properties. At the beginning of the 80's, the group II fluorides of elemental and compound semiconductors received considerable attention[1,3]. Smith *et al.* [4] reported the first metal-epitaxial insulator-semiconductor field-effect transistor (MEISFET) device using CaF_2; SrF_2 and BaF_2 have also been reported [5–8]. However, the water solubility of these fluorides might complicate device processing. The members of the lanthanide fluoride family (XF_3, where X = La, Ce, Pr, Nd, Pm) are water insoluble, mechanically harder, and have significantly smaller thermal expansion coefficients than the group II fluorides. These favorable properties make them attractive candidates for application as protective optical coatings, in MEISFET devices, and in silicon-insulator-silicon structures[9–11].

In these applications the fluoride surfaces may be subjected to irradiation of intense fluxes of both photon and particles. If the irradiation is by heavy ions such as those commonly used in ion implantation, then the surface is eroded by collisional sputtering [12].

In this work we present the results obtained from the 7 keV Ar ion irradiation with fluences of 10^{16}–10^{18} ions/cm^2 of NdF_3 thin films deposited on carbon substrates. The

*Work supported in part by DGAPA-UNAM under contract IN-105489-IF.

changes in film thickness were analysed by measuring fluorine using the resonance in the $^{19}F(p,\alpha\gamma)^{16}O$ nuclear reaction at 340 keV proton energy, and detecting neodymium by using Particle Induced X-ray Emission quantifying the Nd L_α X-rays.

2. EXPERIMENTAL PROCEDURE

2.1 Film deposition and irradiation

Thin films of neodymium fluoride were prepared by vacuum deposition of NdF_3 powder supplied by Aldrich Chem Co. (Milwaukee, Wi., USA), at a working pressure of 3×10^{-6} torr. The films were evaporated onto polished graphite planchettes and cleaned in an ultrasonic bath with acetone and methanol. The planchettes were held at a distance of about 10 cm from the evaporation source. The films showed no good adherence, so the mismatch of the thermal expansion coefficients (about 11×10^{-6} K^{-1} for NdF_3 and 3.5×10^{-6} K^{-1} for graphite) leads to cracking of the film during the contraction of the NdF_3 during cooling following growth.

The samples were placed in a sample holder in the center of the irradiation chamber, which is connected to a 700 keV Van de Graaff accelerator at the Instituto de Física, UNAM. Opposite to the accelerator an ion gun that produces an argon beam with energies up to 10 keV was connected. The sample holder can be rotated in order to irradiate the samples with a 7 keV argon beam and then analyse the thickness changes with a proton beam by PIXE [13]. The argon irradiation was done at fluences between 5×10^{16} ions/cm^2 and 1.9×10^{18} ions/cm^2 with a current density of 10 μA/cm^2. The resonant nuclear reaction (RNRA) was carried out in another chamber.

2.2 Thin Film Analysis

In order to define the film stoichiometry, Rutherford backscattering of 2 MeV He ions was used. One of the spectra taken at the 5.5 MeV Van de Graaff accelerator at the Instituto de Física, UNAM is shown in Fig. 1. The measured stoichiometry was practically NdF_3. The film thickness in μg/cm^2 obtained by this method was compared to the thickness obtained with a Dektak profilometer in nm. From this comparison a density of 2.75 g/cm^3 was calculated. The film thickness change produced by the Ar irradiation was separately determined for the neodymium and for the fluorine.

Three 100 μg/cm^2 NdF_3 films were Ar irradiated with fluences of 5×10^{16} ions/cm^2, 7×10^{16} ions/cm^2 and 12×10^{16} ions/cm^2 respectively. The neodymium thickness change was measured *in situ* with PIXE. In another chamber, the fluorine thickness change was measured by the resonance in the $^{19}F(p,\alpha\gamma)^{16}O$ nuclear reaction at 340 keV proton energy. The 6.14 MeV gamma rays plus first and second escape peaks were measured. The thickness changes measured by PIXE were the same as those measured with RNRA, within the resolution of the two methods (Table I).

A fourth sample, 367 μg/cm^2 thick, was alternately irradiated with Ar ions and measured with PIXE *in situ*. The Ar fluences were 8.6×10^{16} ions/cm^2 to 1.9×10^{18} ions/cm^2. The thickness changes analysed by PIXE are shown in Table II.

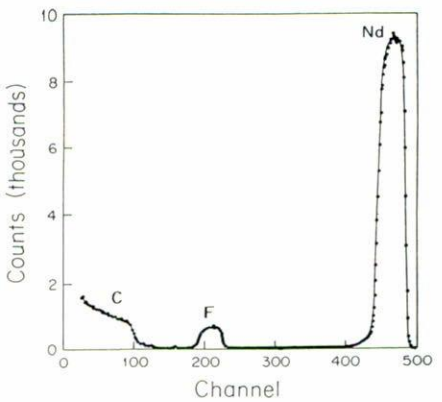

FIGURE 1. 2MeV He^+ RBS spectrum of a 100 $\mu g/cm^2$ NdF_3 film.

TABLE I. Thin film thickness measurements (t) of samples 1, 2 and 3, by different methods, for several ion fluences.

	t_{virgin} ($\mu g/cm^2$)			t_{irrad} ($\mu g/cm^2$)		Fluence (10^{16} ions/cm^2)	Δt ($\mu g/cm^2$)
	RBS	PIXE	RNRA	PIXE	RNRA		
Sample 1	103 ± 7	107 ± 13	111 ± 10	63 ± 4	63 ± 7	5	44 ± 12
Sample 2	101 ± 7	101 ± 11	—	—	47 ± 8	7	55 ± 13
Sample 3	100 ± 7	98 ± 6	96 ± 11	24 ± 2	26 ± 11	12	72 ± 6

TABLE II. Thickness and thickness changes of sample 4 for different ion fluences.

Fluence (10^{16} ions/cm^2)	0	8.6	30.0	70.0	118.0	191.0
t ($\mu g/cm^2$)	367 ± 44	300 ± 24	275 ± 25	263 ± 26	209 ± 19	156 ± 18
Δt ($\mu g/cm^2$)	—	67 ± 13	92 ± 18	104 ± 21	158 ± 31	211 ± 41

2.3 Proton Induced X-ray Analysis (PIXE)

Low energy PIXE ($E_p < 1$ MeV) is a useful tool in thin film thickness determination [17]. Depth information can be obtained, because the ionization cross section drops steeply in this energy region as the proton energy decreases, so the emission of the characteristic X-rays is very sensitive to incident energy changes. Several methods based on the variation of the proton beam incident energy have been proposed and the film thickness changes can be determined within some $\mu g/cm^2$ precision [13]. In the case of NdF_3 film thickness measurement, the Musket and Bauer method [14] is recommended. This procedure compares the number of X-ray photons emitted by the film to that produced by a thick target with the same composition. The ratio C of these two quantities is

$$C = \frac{N_{X,F}}{N_{X,S}} = \frac{\int_0^{t_0 \sec\phi} \sigma_x(E(x)) e^{-\mu x \sec\theta}\, dx}{\int_0^{x \sec\phi} \sigma_x(E(x)) e^{-\mu x \sec\theta}\, dx}, \tag{1}$$

where $\sigma_x(E(x))$ is the X-ray production cross section as a function of the proton energy $E(x)$, which depends on the depth x, μ is the mass absorption coefficient, t is the film thickness, x_0 is the depth at which no more X-rays are produced inside the standard, and ϕ and θ are the angles between the normal to the target surface and the incident direction, and the detector direction, respectively. The subscripts F and S refer to the film and the thick standard. Numerical evaluation of Eq. (1) can be done for different proton incident energies in order to obtain curves that are used to compute the film thickness when C has been measured in the sample.

2.4 Resonant nuclear reaction analysis (RNRA)

The nuclear resonant reaction analysis (RNRA) has been extensively used for determining the presence of elements in materials and their concentration as a function of depth within the material. The $^{19}\mathrm{F}(\mathrm{p},\alpha,\gamma)^{16}\mathrm{O}$ nuclear reaction has very high resonant cross section, and a resonance at 340 keV proton energy is a very convenient way to determine fluorine with a high sensitivity at low proton energies. The resonance width is 2.4 keV, which exceeds both the incoming beam energy spread (typically 1 keV) and the expected Doppler effect, so a simplified calculation of the number of gamma rays can be made [15]:

$$N(E_0) = \int\int C(X)\sigma_{\mathrm{r}}(E)W(E_0, E, x)\,dx\,dE, \tag{2}$$

where $C(x)$ is the depth profile, $\sigma_{\mathrm{r}}(E)$ the cross section for the reaction, and $W(E_0, E, x)$ is the probability that a proton of incoming energy E_0 has energy E at depth x. A desktop computer calculation has been developed where the cross section is taken as a classical Breit-Wigner shape centered at 340 bombarding energy, and the energy probability function is assumed Gaussian [16].

3. RESULTS AND DISCUSSION

The thickness change measured by PIXE was calculated using Eq. (1); the procedure used is described in [17]. The L_α line of Nd was used to quantify the X-ray production. A typical set of C ratio curves obtained by this method is shown in Fig. 2, corresponding to sample 1.

The RNRA analysis was carried out using Eq. (2) calculated by the computer program described in Ref. [16]. An example of the excitation curves obtained is shown in Fig. 3, which also corresponds to sample 1. In both cases, for virgin and irradiated samples, the measured excitation curve has a more extended high energy fall-off than the calculated one, with proton energy straggling considered. This smeared fall-off has been interpreted as the substrate surface roughness. The carbon planchettes were polished, but the ultrasonic bath produced a pockmarked surface. The deviations away from the mean surface height were estimated about 0.5 μm.

The results obtained by the PIXE and RNRA methods for Ar fluences between 5×10^{16} ions/cm^2 and 12×10^{16} ions/cm^2 for different samples of 100 μg/cm^2 are shown

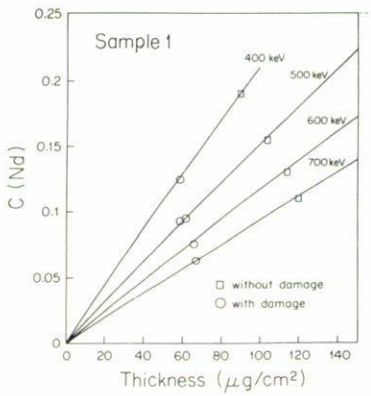

FIGURE 2. Curves of the ratio C of Eq. (1) for the neodymium L_α line, induced by 400–700 keV protons. Experimental points for a virgin and a damaged 100 $\mu g/cm^2$ film are also shown.

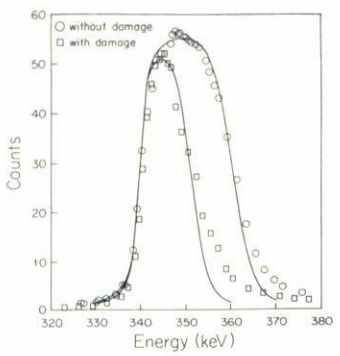

FIGURE 3. Excitation curves for the 340 keV resonance of the reaction $^{19}F(p,\alpha\gamma)^{16}O$, proceduced by a 100 $\mu g/cm^2 NdF_3$ film. The solid curve is a computer calculation of Eq. (2).

in Table I. The thickness change for fluorine and neodymium are the same within the respective resolutions. If there is preferential sputtering, it only produces composition changes in a surface layer with a thickness corresponding with the Ar^+ ions range of about 4 $\mu g/cm^2$. Then, this altered layer has a smaller thickness than the method's resolution, and cannot be observed. Fig. 4 shows the film thickness for the different Ar fluences.

The fourth sample 367 $\mu g/cm^2$ thick, presents a different behaviour and Table II shows the results. The different thickness, measured only by PIXE for the different Ar^+ fluences, are shown in Fig. 5. The film thickness changes Δt for the four samples are shown in Fig. 6.

The Δt changes of the films are due to the sputtering process of the Ar ions on the NdF_3. This sputtering process in most of materials is due to collisional mechanisms. Nevertheless NdF_3 is known to be an insulator, then it is to think that thermal effects and electronic sputtering can contribute to the total sputtering. In insulators, lifetimes of excited states may be long enough to allow excitation energy to be transferred to atomic motion. There are numerous ways of how this can be accomplished in detail, a prototype is the excitation of the bounding ground state of a molecule into an antibonding excited state. Dissociation occurs if the lifetime of the antibonding state is comparable to or greater than the time it takes the nuclei to separate under their mutual repulsive interaction[20]. In some cases,

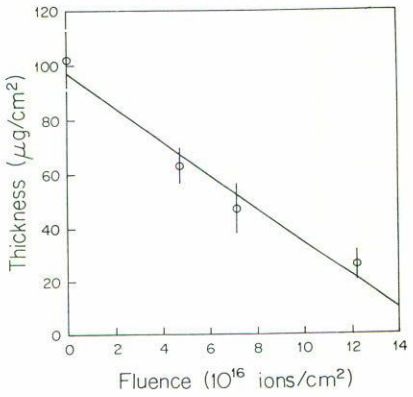

FIGURE 4. Thin film thickness deduced by PIXE and RNRA for Ar^+ fluences between 5×10^{16} ions/cm^2 and 12×10^{16} ions/cm^2 in a 100 μg/cm^2 film thickness.

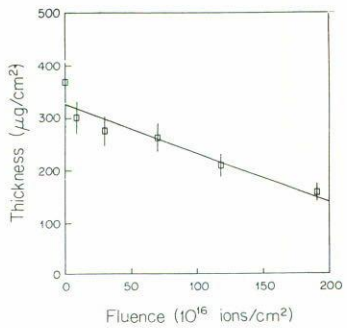

FIGURE 5. Same as Fig. 4, but for Ar^+ fluences of 8.6×10^{16} ions/cm^2 and 1.9×10^{18} ions/cm^2 in a 367 μg/cm^2 film thickness.

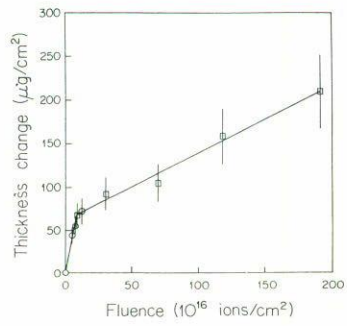

FIGURE 6. Thin film thickness changes for Ar^+ fluences from 5×10^{16} ions/cm^2 up to 1.9×10^{18} ions/cm^2 in both films thicknesses.

like alkali halides, the sputtering yields measured are dominated by this process when the proyectile energy is enough. Energy distribution measurements for NaCl indicate that for high electronic stopping power sputtering is dominated by electronic processes, but when the nuclear stopping begins to increase the collisional sputtering become important[19]. For 7 keV Ar ions on NdF_3 the nuclear stopping power is about eight times higher than

the electronic one. Furthermore, electronic mechanism frequently only removes a single element from a compound, which was not observed. However, with the methods used the electronic contribution to the thickness change cannot be estimated.

If we assume that the principal process is collisional, then the topography of the film surface can determine the sputtering yield value. We have observed that NdF_3 thin films grown on carbon planchettes present different surface topography for different thicknesses due to poor adherence and thermal process. Then this fact suggests that the different Δt slopes are due to topography effects [21].

Calculations with the program TRIM [18] predict that the atoms are removed stoichiometrically in the linear cascade regime. Although the fluorine sublimation energy is not known, the same proportion of the sputtered atoms is calculated for any surface binding energy. The PIXE and RNRA methods measure the neodymium and fluorine thickness respectively, and are in agreement with the TRIM calculation within the resolution of the two methods.

Since no changes in the film composition were found in a first approximation, the sputtering yield may be calculated for molecules removed per incident ion from the change of the film thickness:

$$Y = N \frac{\Delta t}{F}, \tag{3}$$

where N is the number of molecules per cm^3, and F the ion fluence. Fig. 6 shows a linear behavior for each of the two sets of data. From the corresponding slopes, two sputtering yields can be obtained: $Y = 1.7$ mol/ion and $Y = 0.2$ mol/ion for the 100 $\mu g/cm^2$ and 367 $\mu g/cm^2$ thickness, respectively, with an uncertainty of 15%.

ACKNOWLEDGEMENT

The authors thank K. López, J.C. Pineda, and E. Pérez Zavala, for the operation and maintenance of the 0.7 MeV and 5.5 MeV accelerators.

REFERENCES

1. R.F.C. Farrow, P.W. Sullivan, G.M. Williams, G.R. Jones and D.C. Cameron. *J. Vac. Sci. Technol.* **19** (1981) 415.
2. H. Ishiwara and T. Asano, *Appl. Phys. Lett.* **40** (1982) 66.
3. S. Sinharoy, R. A. Hoffman, J.H. Rieger, R.F.C. Farrow and A.J. Noreika, *J. Vac. Sci. Technol.* **A3** (1985) 842.
4. T.P. Smith III, J.M. Phillips, W.M. Augustyniak and P.J. Stiles, *Appl. Phys. Lett.* **45** (1984) 907.
5. H. Ishiwara, T. Asano and S. Furukawa, *J. Vac. Sci. Technol.* **B1** (1983) 266.
6. C.W. Tu, S.R. Forrest and W.D. Johnston, Jr., *Appl. Phys. Lett.* **43** (1983) 569.
7. S. Siskos, C. Fontaine and A. Munoz-Yague, *Appl. Phys. Lett.* **44** (1984) 1146.
8. P.W. Sullivan, G.M. Metze and J.E. Bower, *J. Vac. Sci. Technol.* **B3** (1985) 500.
9. V.S. Dharmadhikari, *J. Appl. Phys.* **54** (1983) 4087.

10. S. Sinharoy, R.A., Hoffman, R.F.C. Farrow and J.H. Rieger, *J. Vac. Sci. Technol.* **A3** (1985) 2323.
11. P.G. McMullin and S. Sinharoy, *J. Vac. Sci. Technol.* **A6** (1988) 1367.
12. P. Sigmund, *Phys. Rev.* **184** (1969) 393; and in *Sputtering by Particle Bombardment*, vol. 1, ed. R. Behrisch, Springer, Berlin, (1981), p. 9
13. J. Miranda, A. Oliver, F.J. Ruiz and J.M. Santana, Int. J. PIXE **1** (1991) 259.
14. R.G. Muskert and W. Bauer, *J. Appl. Phys.* **43** (1972) 4786.
15. G. Amsel, J.P. Nadai, E. D'Artemare, D. David, E. Girard and J. Moulin, *Nucl. Instr. and Meth* **92** (1971) L181.
16. J. Rickards, *Nucl. Instr. and Math in Phys. Res.* **B56/57** (1991) 812.
17. J. Rickards, A. Oliver, J. Miranda and E.P. Zironi, *Appl. Surf. Sci.* **45** (1990) 155.
18. J.P. Biersack and L.G. Haggmark, *Nucl. Instr. and Meth* **174** (1980) 257.
19. W. Husinsky and R. Bruckmuller, *Surf. Sci.* **80** (1979) 637.
20. P.C. Towsend in *Sputtering by Particle Bombardment*, vol. 2, Chap. 4, Springer, Berlin, (1983), p. 147.
21. U. Littmark, W. Hofer, *J. Mater. Sci.* **13** (1978) 2577.